VSWR is given by

$$\text{VSWR}\,|_{g=\infty} = \frac{1 + |\Gamma'|}{1 - |\Gamma'|} = \frac{1 + ||r_s| - \rho_s|}{1 - ||r_s| - \rho_s|} = S.$$

Let $b = ||r_s| - \rho_s|$, and if ν equals maximum tolerable deviation of the VSWR of the system.

$$\text{VSWR}\,|_{\text{stable}} = (1 - 2\nu)S = S'$$

giving

$$|\Gamma| = \frac{2\nu(1 + b) - b}{2 - 2\nu(1 + b)}.$$

By definition, $|\Gamma| = M\,|r_s| - \rho_s| = M \cdot b$

$$M = \frac{2\nu(1 + 1/b) - 1}{2 - 2\nu(1 + b)}$$

$$= \frac{\nu(1 + (||r_s| - \rho_s|)^{-1}) - 0.5}{1 - \nu(1 + ||r_s| - \rho_s|)}.$$

Appendix II

Reflection Detuning Factor

The detuning factor δ_r is defined as the fractional change in the two-port input reflection coefficient with respect to the fractional change in the output load reflection coefficient, i.e.,

$$\delta_{r2} = \left(\frac{\partial \Gamma_1}{\Gamma_1}\right) \bigg/ \left(\frac{\partial r_2}{r_2}\right).$$

But

$$\Gamma_1 = S_{11} - \frac{S_{12}S_{21}}{S_{22} - (1/r_2)} = \frac{S_{11} - r_2\Delta}{1 - r_2S_{22}}$$

$$\frac{\partial \Gamma_1}{\partial r_2} = \frac{S_{12}S_{21}}{[S_{22} - (1/r_2)]^2} \cdot \frac{1}{r_2^2}$$

$$\delta_{r2} = \frac{S_{12}S_{21}}{(1 - r_2S_{22})^2} \cdot \frac{r_2/(S_{11} - r_2\Delta)}{1 - r_2S_{22}}$$

$$\delta_{r2} = \frac{r_2S_{12}S_{21}}{(1 - r_2S_{22})(S_{11} - r_2\Delta)}.$$

Hence for a specified value of δ_{r2}

$$S_{11} - r_2\Delta - r_2S_{11}S_{22} + r_2^2\Delta S_{22} - \frac{r_2}{\delta_{r2}} S_{12}S_{21} = 0$$

$$|r_2| = \left|\left(\frac{\Delta + S_{11}S_{22} + (S_{12}S_{21})/\delta_{r2}}{2 . S_{22} . \Delta}\right) \pm \left|\left(\frac{\Delta + S_{11}S_{22} + (S_{12}S_{21})/\delta_{r2}}{2 . S_{22} . \Delta}\right)^2 - \left(\frac{S_{11}}{S_{22}\Delta}\right)\right|^{1/2}\right|.$$

This is the limiting value of the load reflection coefficient.

References

[1] D. Leed and O. Kummer, "A loss and phase set for measuring transistor parameters and two-port networks between 5 and 250 MHz," *Bell Syst. Tech. J.*, pp. 841–884, May 1961.
[2] D. Leed, "An insertion loss, phase and delay measuring set for characterizing transistors and two-port networks between 0.25 and 4.2 GHz," *Bell Syst. Tech. J.*, pp. 194–202, Mar. 1966.
[3] F. Weinert, "Scattering parameters speed design of high-frequency transistor circuits," *Electronics*, vol. 40, pp. 78–88, Sept. 5, 1966.
[4] W. H. Froehner, "Quick amplifier design with scattering parameters," *Electronics*, vol. 41, pp. 100–109, Oct. 16, 1967.
[5] M. F. Abulela, "A study of linear integrated circuits," M.S. thesis, Manchester Univ., Manchester, England, ch. 4, pp. 74–86, Oct. 1970.
[6] K. Kurokawa, "Power waves and the scattering matrix," *IEEE Trans. Microwave Theory Tech.*, vol. MTT-13, pp. 194–202, Mar. 1965.
[7] G. Bodway, "Two-port power flow analysis using generalized scattering parameters," *Microwave J.*, vol. 10, pp. 61–69, May 1967.
[8] A. P. Stern, "Stability and power gain of tuned transistor amplifiers," *Proc. IRE*, vol. 45, pp. 335–343, Mar. 1957.
[9] J. M. Rollett, "Stability and power gain invariants of linear two-ports," *IRE Trans. Circuit Theory*, vol. CT-9, pp. 29–32, Mar. 1962.
[10] M. F. Abulela, "Studies of some aspects of linear amplifier design in terms of measurable two-port and three-port scattering parameters," Ph.D. dissertation, Manchester Univ., Manchester, England, 1972.
[11] C. S. Gledhill and M. F. Abulela, "Notes on the conjugate matched two-port as a UHF amplifier," *IEEE Trans. Microwave Theory Tech.*, vol. MTT-20, pp. 289–292, Apr. 1972.
[12] J. G. Linvill and J. F. Gibbons, *Transistors and Active Circuits*. New York: McGraw-Hill, 1961.

Equivalent Circuits of Microstrip Impedance Discontinuities and Launchers

J. S. WIGHT, STUDENT MEMBER, IEEE, O. P. JAIN, W. J. CHUDOBIAK, MEMBER, IEEE, AND V. MAKIOS, MEMBER, IEEE

***Abstract*—Experimental results obtained indicate that an excess phase shift is the most pronounced high-frequency parasitic effect resulting from a microstrip quarter-wave transformer impedance discontinuity. An empirically derived design-oriented model describing the dominant parasitic reactances associated with a microstrip impedance discontinuity at *X*-band frequencies is described. A description is also given of the dominant parasitic reactances associated with a number of commercially available coaxial-to-microstrip launchers.**

I. Introduction

A number of authors [1]–[3] have considered the parasitics associated with impedance discontinuities (such as quarter-wave transformers) in stripline transmission lines. However, very little has been reported concerning impedance discontinuities in microstrip transmission lines [4]. Experimental results obtained by the present authors indicate that an excess phase shift is the most pronounced high-frequency parasitic effect resulting from impedance discontinuities such as in quarter-wave transformers. An empirically derived design-oriented model describing the dominant parasitic reactances associated with a microstrip impedance discontinuity at *X*-band frequencies is described in this short paper. The model is based on the stripline impedance discontinuity analysis reported by Altschuler and Oliner [1], the effective linewidth analysis reported by Leighton and Milnes [4], and the open-circuited transmission line analyses by Altschuler and Oliner [1] and Jain *et al.* [5]. It is shown that the model is valid for characteristic impedance values ranging from 10 to 130 Ω. A description is also given of the dominant parasitic reactances associated with a number of commercially available coaxial-to-microstrip launchers in high VSWR applications (VSWR > 2). The technique used to characterize the launchers is similar to that reported by Weissfloch [6], except that the equivalent-circuit form and parameter values are determined using a simple graphical technique.

II. Experimental Techniques and Launcher Equivalent Circuits

The experimental data reported in this short paper were obtained using structures of the form shown in Fig. 1 and the HP 8410 network analyzer. Published ϵ_{eff} models [7], [8] and experimental resonant ring techniques [9] were used to accurately determine the effective electrical lengths of the various sections of the transformer structures. Traveling microscope measurements of a tolerance of

Manuscript received September 13, 1972; revised June 22, 1973. This work was supported in part by the Canadian Department of Communications under Research Contract OGR2-0073.
J. S. Wight and V. Makios are with the Faculty of Engineering, Carleton University, Ottawa, Ont., Canada.
O. P. Jain was with the Faculty of Engineering, Carleton University, Ottawa, Ont., Canada. He is now with Radio Corporation of America Ltd., Ste. Anne de Bellevue, P.Q., Canada.
W. J. Chudobiak is with the Department of Communications, Communications Research Centre, Ottawa, Ont., Canada.

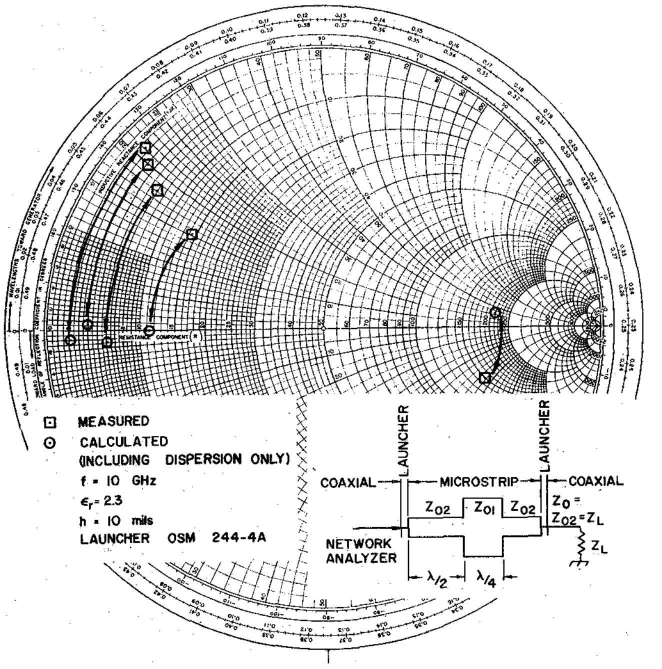

(a)

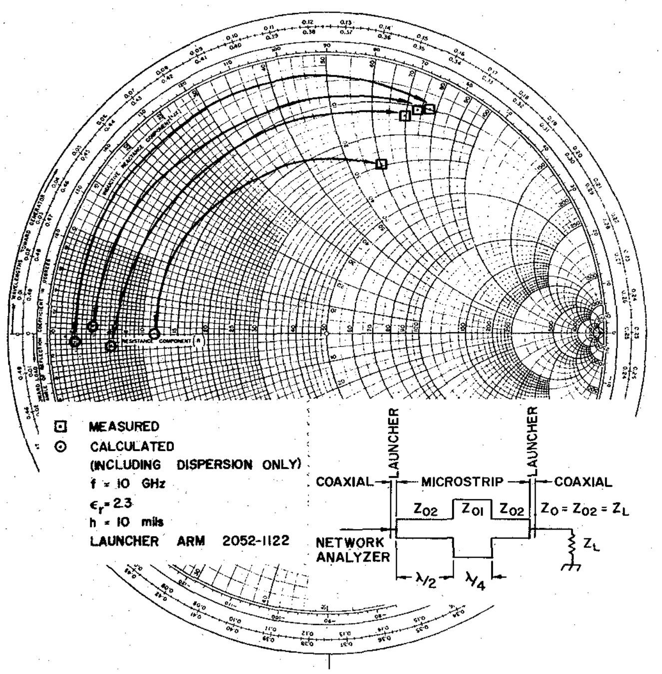

(b)

Fig. 1. Measured and calculated impedance values (including only dispersion) for transformer structures on thin plastic substrates (f = 10 GHz, ϵ_r = 2.3, h = 10 mil). (a) Launcher OSM 244-4A. (b) Launcher ARM 2052-1122.

$\pm 0.001\lambda$ were conducted and deviations from the required dimensions were accounted for.

Measured and calculated transformed impedance values for a number of different transformer structures on substrates of various thicknesses and dielectric constants and utilizing a number of different launchers are compared in Fig. 1 and Tables I and II. It is seen in Fig. 1 that the measured load reactance value varies with the type of microstrip launcher used. A two-element equivalent circuit of the launcher reactive parasitics is developed in this section using a simple graphical–experimental technique rather than Weissfloch's

TABLE I

Measured and Calculated Load Impedance Values for Transformer Structures (See Fig. 1) on Alumina Substrates (f = 10 GHz, ϵ_r = 9.9, h = 10 mil) Using Launcher OSM 244-4A

Characteristic Impedance of Transformer Section Z_{01} (Ω)	9.7	11.5	14.8	19.9
Measured	2.1 + j23	3.0 + j18	4.6 + j23	8.5 + j20
Calculated (including dispersion only)	1.8 + j1.3	2.5 − j3.5	4.3 + j4.5	8.6 + j3.5
Calculated (including dispersion and launcher parasitics)	2.0 + j16	2.5 + j11	4.0 + j19.6	9.6 + j19.4
Calculated (including dispersion, launcher parasitics, and impedance discontinuity parasitics)	2.0 + j22	3.1 + j16.2	4.5 + j22.4	9.6 + j22

TABLE II

Measured and Calculated Load Impedance Values for Transformer Structures (See Fig. 1) on Thin Plastic Substrates (f = 10 GHz, ϵ_r = 2.3, h = 10 mil) Using Launcher ARM 2052-1122

Characteristic Impedance of Transformer Section Z_{01} (Ω)	10.1	16.5	17.6	23
Measured	10 + j78	11 + j74	14 + j70	29 + j60
Calculated (including dispersion only)	2.4 − j0.8	4.2 + j0.9	6.2 − j1.5	11.6 + j0.0
Calculated (including dispersion and launcher parasitics)	6.0 + j54	13 + j56	18 + j49	34 + j46
Calculated (including dispersion, launcher parasitics, and impedance discontinuity parasitics)	11 + j80	14 + j68	23 + j64	38 + j53

[6] iterative technique, which yields a three-element equivalent circuit.

The launcher characterization technique consists of using the launcher to make input impedance measurements on various lengths of open-circuited 50-Ω line ($\lambda/8 < L < \lambda$). The measurement procedure differs from Weissfloch's to the extent that the measurement point and the reference plane coincide, thus eliminating the requirement for an analytical transformation.

The variation of the excess phase angle (measured input reflection-coefficient phase angle minus calculated input reflection-coefficient phase angle) versus the electrical length of the open-circuited line is shown in Fig. 2(a). The cyclical variation (within experimental error limits) exhibited in Fig. 2(a) may be used to synthesize a two-element equivalent circuit of the launcher [Fig. 2(b)] using the following argumentation. It is evident from a consideration of a transmission line immittance chart that for measured input reflection-coefficient phase angles in the range of say $\pm 30°$, the phase angle is relatively insensitive to variations of series reactance at the reference plane, while the phase angle is extremely sensitive to variations of the shunt reactance at the reference plane.

Similarly, it is seen that for input reflection-coefficient phase angles of $180 \mp 30°$, the phase angle is relatively insensitive to variations of the shunt reactance, while being extremely sensitive to variations of the series reactance. The equivalent circuit shown in Fig. 2(b) follows from the knowledge that the excess phase angle at a line length of $\lambda/2$ is due almost entirely to the launcher shunt capacitance, while at $\lambda/4$ it is due almost entirely to the launcher series inductance, a constant phase value in both cases being accounted for by the open-end effect [5], [10]–[12]. Numerical values

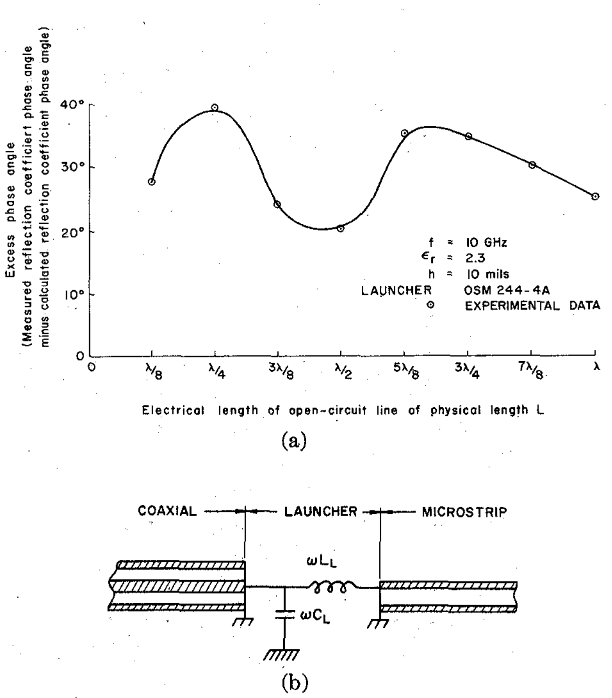

Fig. 2. (a) Excess phase angle for an open-circuited line determined using an OSM 244-4A launcher (f = 10 GHz, ϵ_r = 2.3, h = 10 mil). (b) Equivalent circuit of the microstrip launcher interface.

for ωL_L and ωC_L can be conveniently obtained by plotting the experimental data, as shown in Fig. 3(a), and superimposing the data for the electrical lengths $\lambda/4$ and $\lambda/2$ on a transmission line chart, as shown in Fig. 3(b). The ωL_L and ωC_L values at 10 GHz for typical launcher/substrate combinations are tabulated in Table III.

The calculated transformed load impedance values shown in Fig. 1(a) (which do not include either launcher or impedance discontinuity parasitic reactances) are reproduced in Fig. 4(a), along with calculated impedance values which include the effect of the aluncher parasitics. Similar data are represented in Fig. 4(b) for another common launcher/substrate combination. From Fig. 4 (and Tables I and II) it is seen that even with the inclusion of the launcher parasitics, there remains an excess phase shift between measured and predicted impedance values. Since the launcher characteristics are well understood and since the microstrip wavelength is known to a high degree of accuracy, the remaining excess phase shift can only be due to a reactance associated with impedance discontinuities. An equivalent circuit of a microstrip impedance discontinuity is derived in the following section.

III. Impedance Discontinuity Equivalent Circuit

Parasitic reactances are associated with an impedance discontinuity in a microstrip transmission line since there are longitudinal components of both the electric and magnetic fields. Altschuler and Oliner [1] have shown that the following equation adequately describes the discontinuity series reactance for stripline structures:

$$\omega L = \frac{2Z_{01}W_1^*}{\lambda} \ln\left[\operatorname{cosec}\left(\frac{\pi}{2}\frac{W_2^*}{W_1^*}\right)\right] \tag{1}$$

where

- ωL impedance discontinuity series reactance;
- Z_{01} characteristic impedance of the transformer section;
- $W_{1,2}^*$ equivalent stripwidth;
- λ wavelength.

The results reported later in this short paper indicate that this equation also adequately describes the discontinuity series reactance for microstrip transmission line structures, provided that the equivalent stripwidth terms W_1^* and W_2^* are represented by the following

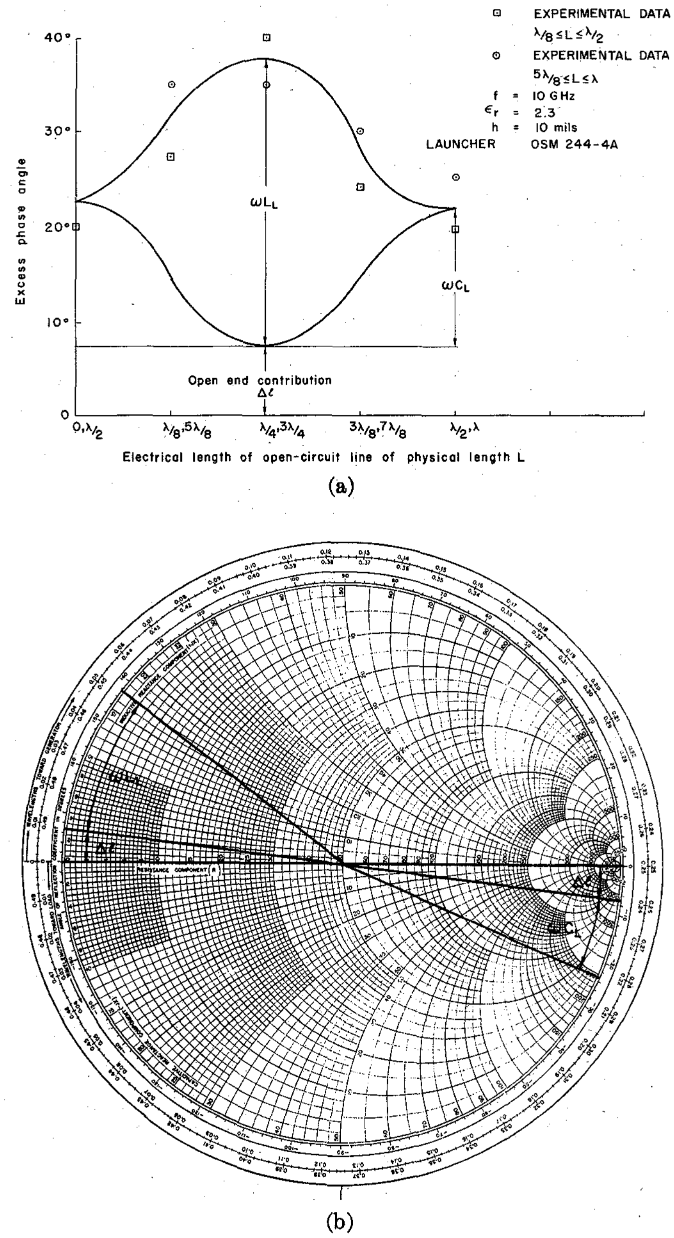

Fig. 3. (a) Graphical determination of launcher equivalent-circuit parameters from excess phase-angle plots for an open-circuited line with an OSM 244-4A launcher at 10 GHz (ϵ_r = 2.3, h = 10 mil). Experimental points for $\lambda/2 \le L \le \lambda$ superimposed on points for $\lambda/8 \le L \le \lambda/2$. (b) Graphical technique for determining numerical values of launcher parasitics ωL_L and ωC_L.

TABLE III
Launcher Equivalent-Circuit Parameters for Various Launcher/Substrate Combinations at 10 GHz

Substrate \ Launcher	OSM 244-4A		ARM 2052-1124	
	ωL_L (Ω)	ωC_L (mmho)	ωL_L (Ω)	ωC_L (mmho)
ϵ_r = 2.3, h = 10 mil	14.2	2.9	31	14.5
ϵ_r = 9.9, h = 25 mil	9.0	1.1	50	7.0
ϵ_r = 9.9, h = 10 mil	14.5	2.3	60	8.0

expression for microstrip reported by Leighton and Milnes [4]:

$$W_n^* = \frac{hR_c}{Z_{0n}}\left(\frac{1}{\epsilon_{\text{eff}}}\right)^{1/2}, \qquad (n = 1,2) \tag{2}$$

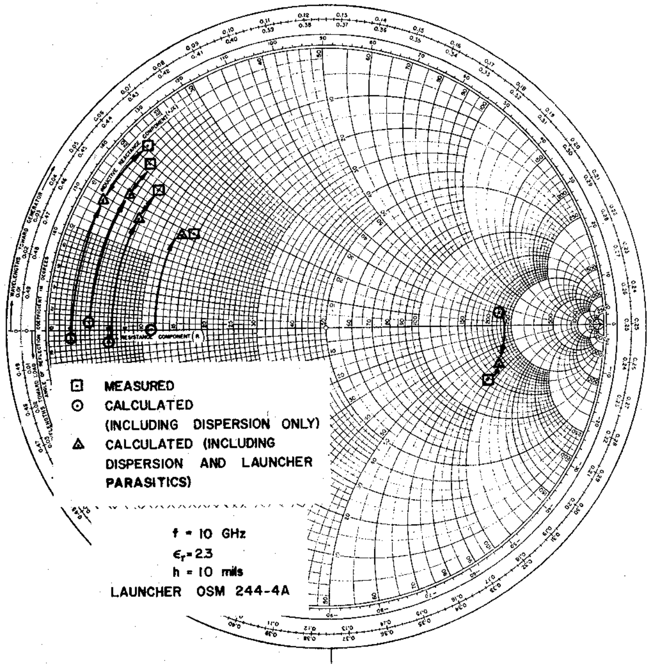

(a)

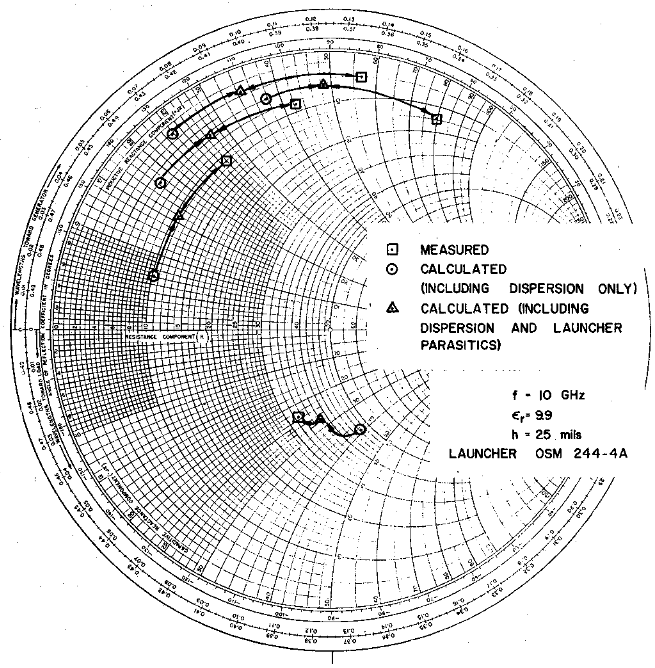

(b)

Fig. 4. Measured and calculated impedance values (including either only dispersion or dispersion and launcher parasitics as indicated) for transformer structures on plastic and alumina substrates at 10 GHz. (a) Launcher OSM 244-4A, $\epsilon_r = 2.3$, $h = 10$ mil. (b) Launcher OSM 244-4A, $\epsilon_r = 9.9$, $h = 25$ mil.

where

- h substrate thickness;
- R_c free-space wave impedance;
- ϵ_{eff} effective dielectric constant of the microstrip transmission line;
- Z_{01} characteristic impedance of quarter-wave transformer section (see Fig. 5);
- Z_{02} characteristic impedance of lines adjacent to transformer section (see Fig. 5).

The effect of a longitudinal component of the electric field for an open-circuited stripline has been described by Altschuler and Oliner [1] as an apparent increase of the line length. Farrar and Adams [10] have shown, using numerical techniques, that the effect of the longitudinal line component of the electric field at a microstrip impedance discontinuity may be represented as a shunt capacitance. The present authors have found that if the microstrip impedance step discontinuity is approximated by an open circuit, then the following equation first given by Altschuler and Oliner [1] may be used to account for the longitudinal component, provided that the ground-plane separation term b is replaced by $2h$ in the expression for the parameter C as shown below

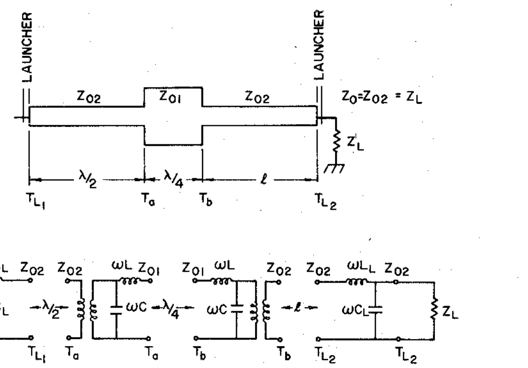

Fig. 5. Equivalent circuits of microstrip transformer impedance discontinuity parasitics (with launcher parasitics).

$$\Delta l = C\left[\frac{C + 2W}{4C + 2W}\right] \tag{3}$$

where

- Δl apparent increase in length of the center conductor due to fringing field;
- W linewidth;
- $C \;= \dfrac{h \ln 4}{\pi}.$

The value given by (3) may readily be converted into an equivalent shunt-susceptance value ωC for application in the impedance discontinuity equivalent circuits shown in Fig. 5. These ωC values agree within ± 0.5 mmho with that predicted by the numerical model of Farrar and Adams [10]. However, as is shown in the following paragraph, the contribution of the ωC parasitic to the overall excess phase shift is small in comparison with the ωL contribution.

The transformed load impedances shown in Fig. 4 are reproduced in Fig. 6 and modified by the addition of the ωL and ωC values given by (1) and (3). It is seen that with the addition of the ωL and ωC effects (primarily the former since it accounts for a much larger excess phase angle), the discrepancy between the two cases shown in Fig. 4 is accounted for very accurately.

Calculated transformed impedance values shown in Fig. 6 account for launcher parasitics, impedance discontinuity parasitics, and dispersion of the microstrip transmission line dielectric constant. The relative importance of the various factors is apparent from Figs. 4 and 7, where it is seen that the effect of dispersion is minimal when compared with that of ωL.

IV. Conclusions

A description is given of a relatively simple experimental–graphical technique which yields a two-element equivalent circuit of the reactive parasitics of a microstrip launcher in a high VSWR line (VSWR > 2) at a specified frequency. It is demonstrated that the reactive parasitics contribute a significant excess phase component (of the order of 20°) to the measured reflection coefficient when the launcher is used in a measurement on a microstrip circuit.

It was also demonstrated that a number of empirically derived equations, originally developed for describing stripline impedance discontinuities, adequately model the reactive parasitics associated with microstrip impedance discontinuities, provided that a number of modifications are performed. The validity of the two-element

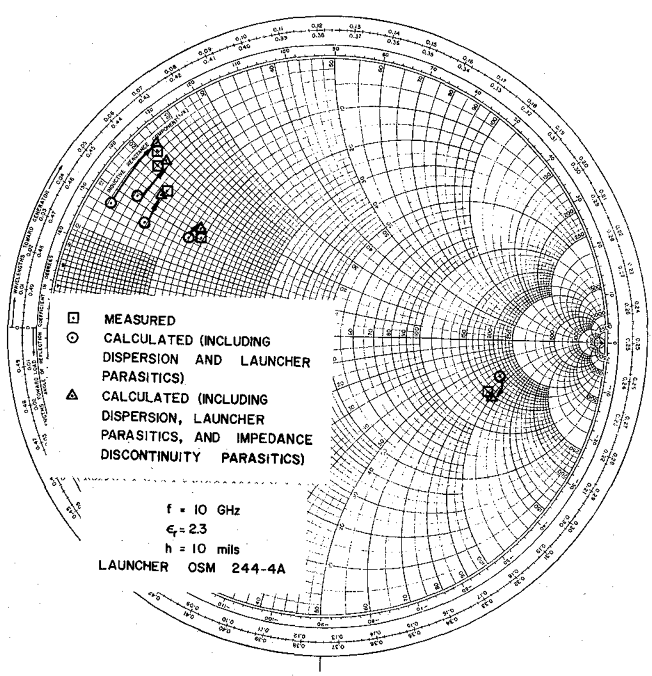

(a)

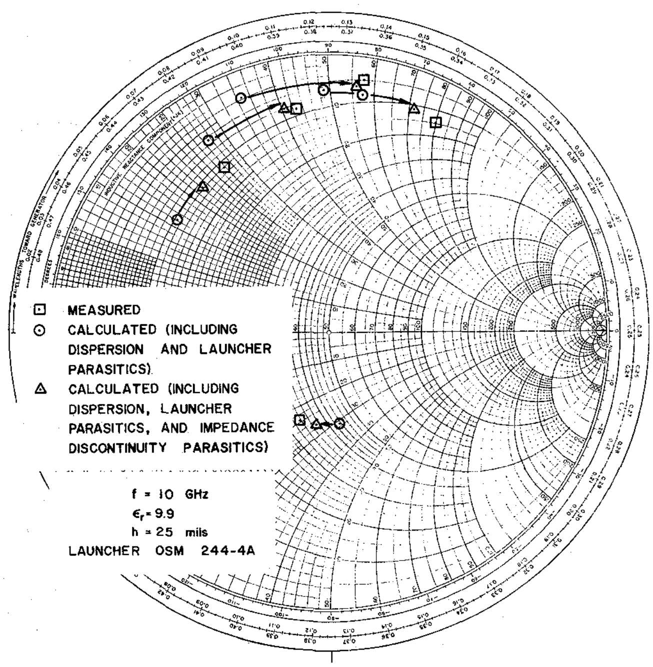

(b)

Fig. 6. Measured and calculated impedance values (including either dispersion and launcher parasitics or dispersion, launcher parasitics, and impedance discontinuity parasitics as indicated) for transformer structures on plastic and alumina substrates at 10 GHz. (a) Launcher OSM 244-4A, $\epsilon_r = 2.3$, $h = 10$ mil. (b) Launcher OSM 244-4A, $\epsilon_r = 9.9$, $h = 25$ mil.

model described by the equations is confirmed using a variety of quarter-wave transformer structures. It is shown that at X-band frequencies, the effect of the impedance discontinuity parasitic reactances is significant, much larger in fact than that of the dispersion of the effective dielectric constant.

References

[1] H. M. Altschuler and A. A. Oliner, "Discontinuities in the center conductor of symmetric strip transmission lines," *IRE Trans. Microwave Theory Tech.*, vol. MTT-8, pp. 328–339, May 1960.

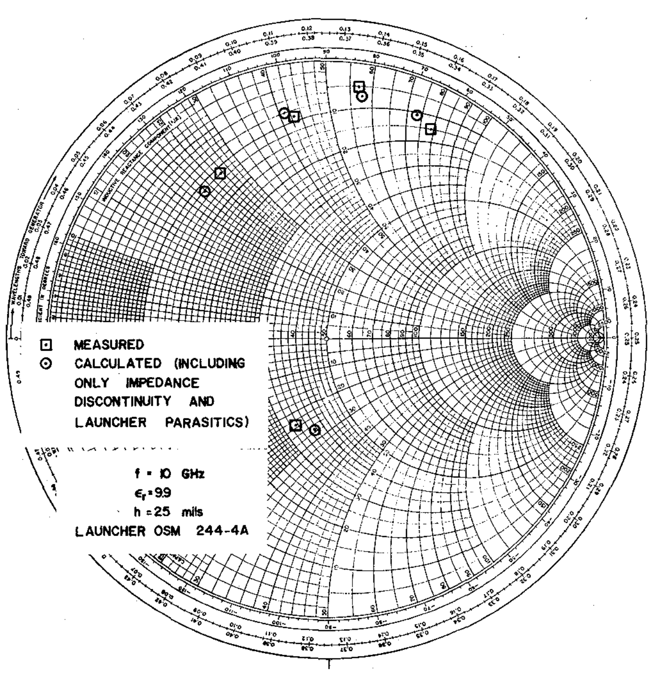

Fig. 7. Measured and calculated impedance values (including only launcher and impedance discontinuity parasitics) for a transformer structure on an alumina substrate ($f = 10$ GHz, $\epsilon_r = 9.9$, $h = 25$ mil).

[2] A. A. Oliner, "Equivalent circuits for discontinuities in balanced strip transmission line," *IRE Trans. Microwave Theory Tech.* (*Special Issue: Symposium on Microwave Strip Circuits*), vol. MTT-3, pp. 134–143, Mar. 1955.
[3] V. Nalbandian and W. Steenaart, "Discontinuities in symmetric striplines due to impedance steps and their compensations," *IEEE Trans. Microwave Theory Tech.*, vol. MTT-20, pp. 573–578, Sept. 1972.
[4] W. H. Leighton, Jr., and A. G. Milnes, "Junction reactance and dimensional tolerance effects on X-band 3-dB directional couplers," *IEEE Trans. Microwave Theory Tech.*, vol. MTT-19, pp. 818–825, Oct. 1971.
[5] O. P. Jain, V. Makios, and W. J. Chudobiak, "Open-end and edge effect in microstrip transmission lines," *IEEE Trans. Microwave Theory Tech.*, vol. MTT-20, pp. 626–628, Sept. 1972.
[6] A. Weissfloch, *Hochfreq. Elektroakust.*, vol. 60, pp. 67 *ff.*, 1972; and N. Marcuvitz, *Waveguide Handbook* (*Mass. Inst. Technol. Rad. Lab. Series*), vol. 10. New York: McGraw-Hill, pp. 130–135.
[7] O. P. Jain, "A study of dispersive behaviour in microstrip transmission lines," Faculty of Eng., Carleton Univ., Ottawa, Ont., Canada, Tech. Rep., May 1971.
[8] W. J. Chudobiak, O. P. Jain, and V. Makios, "Dispersion in microstrip," *IEEE Trans. Microwave Theory Tech.*, vol. MTT-19, pp. 783–784, Sept. 1971.
[9] P. Troughton, "Measurement techniques in microstrip," *Electron. Lett.*, vol. 5, pp. 25–26, Jan. 23, 1969.
[10] A. Farrar and A. T. Adams, "Matrix methods for microstrip three-dimensional problems," *IEEE Trans. Microwave Theory Tech.*, vol. MTT-20, pp. 497–504, Aug. 1972.
[11] D. S. James and S. H. Tse, "Microstrip end effects," *Electron. Lett.*, vol. 8, pp. 46–47, Jan. 1972.
[12] P. Silvester and P. Benedek, "Equivalent capacitances of microstrip open circuits," *IEEE Trans. Microwave Theory Tech.*, vol. MTT-20, pp. 511–516, Aug. 1972.

Microwave Measurement of Dielectric Constant of Liquids and Solids Using Partially Loaded Slotted Waveguide

INDER J. BAHL AND HARI M. GUPTA, STUDENT MEMBER, IEEE

***Abstract*—An accurate method is described for the measurement of the dielectric constant of liquids and solids. The dielectric material partially loads a slotted rectangular waveguide and the guide wavelength is measured for two different thicknesses of the dielectric. The guide wavelengths are related to the dielectric con-**

Manuscript received December 20, 1972; revised June 18, 1973.
The authors are with the Department of Electrical Engineering, Indian Institute of Technology, Kanpur (U.P.), India.